

Thermoelectric properties of a weakly coupled quantum dot: Enhanced thermoelectric efficiency

M. Tsaousidou*

Materials Science Department, University of Patras, Patras 26504, Greece

G.P. Triberis

Physics Department, Solid State Section, University of Athens,
Panepistimiopolis, 15784, Zografos, Athens, Greece

We study the thermoelectric coefficients of a multi-level quantum dot (QD) weakly coupled to two electron reservoirs in the Coulomb blockade regime. Detailed calculations and analytical expressions of the power factor and the figure of merit are presented. We restrict our interest to the limit where the energy separation between successive energy levels is much larger than the thermal energy (i.e., the quantum limit) and we report a giant enhancement of the figure of merit due to the violation of the Wiedemann-Franz law when phonons are frozen. We point out the similarity of the electronic and the phonon contribution to the thermal conductance for zero dimensional electrons and phonons. Both contributions show an activated behavior. Our findings suggest that the control of the electron and phonon confinement effects can lead to nanostructures with improved thermoelectric properties.

PACS numbers: 73.50.Lw, 73.23.Hk, 73.63.Kv

I. INTRODUCTION

The thermoelectric properties of nanomaterials have attracted a great deal of interest in the last few years due to the potential applications in power generation and refrigeration [1]. There is increasing evidence that the thermoelectric performance of nanostructured materials can be significantly improved. The efficiency of a device to convert heat into electricity and vice-versa is measured by the dimensionless figure of merit ZT given by

$$ZT = \frac{S^2GT}{\kappa}, \quad (1)$$

where S is the thermopower, G is the electrical conductance, T is the absolute temperature and κ is the thermal conductance. There are two contributions to κ : the electronic, κ_e , and the phonon, κ_{ph} .

Good thermoelectric materials are considered to be those with $ZT > 3$ at room temperature [2]. The best commercial thermoelectric material is bulk Bi_2Te_3 and its alloys with Sb and Se with ZT close to 1. Although there is no thermodynamic requirement that imposes an upper limit on ZT , until 2001 no progress had been made in increasing ZT above 1. The difficulty is due to the interrelations between the coefficients S , G and κ that set limitations in varying them independently. A characteristic example is the Wiedemann-Franz law according to which the ratio κ_e/GT remains constant.

Since 2000 there has been a number of experiments in nanostructures where the barrier of $ZT = 1$ has been overcome at high temperatures. Venkatasubramanian *et al.* [3] measured $ZT \approx 2.4$ in p -type $\text{Bi}_2\text{Te}_3/\text{Sb}_2\text{Te}_3$ superlattices at $T = 300$ K. The reason for the enhanced

figure of merit is the phonon blocking due to acoustic mismatch between Bi_2Te_3 and Sb_2Te_3 that causes a significant reduction to κ_{ph} . Harman *et al.* [4] reported values of ZT between 1.3 to 1.6 in $\text{PbSeTe}/\text{PbTe}$ quantum dot superlattices. More recently Kanatzidis and co-workers found that bulk $\text{AgPb}_{18}\text{SbTe}_{20}$ with internal nanostructures has $ZT \approx 2$ at $T = 800$ K [5]. In nanocrystalline BiSbTe bulk alloys ZT reached the value 1.4 at $T = 373$ K [6]. The enhanced ZT was attributed to the significant reduction of κ_{ph} due to the strong phonon scattering by the interfaces between the nanostructures. A 100-fold improvement of ZT compared to the bulk value has been reported recently in Si nanowires [7, 8]. In [7] the increased ZT is due to particularly small values of κ_{ph} that reach the amorphous limit, while in [8] the phonon-drag effect [9, 10] was identified as the reason for the increased thermopower at $T = 200$ K.

Early theoretical work pointed out the possibility of enhancing ZT in structures of reduced dimensionality due to the increased density of states near the Fermi level [11]. Mahan and Sofo [12] predicted a maximization of the thermoelectric efficiency in materials with a delta-like density of states. This suggests that quantum dots and molecular junctions are promising candidates for good thermoelectric materials. Humphrey and Linke [13] provided a thermodynamic explanation why the optimum density of states for enhanced ZT is a delta function. More recent theoretical studies [14–18] point out the possibility of significantly improving the thermoelectric efficiency in small quantum dots and molecules.

The present work presents a comprehensive analysis of the thermoelectric properties of a weakly coupled multi-level quantum dot (QD) in the sequential tunneling transport regime and suggests the possibility of a huge increase of ZT in the Coulomb blockade regime due to the violation of the Wiedemann-Franz law. We focus on the quantum limit where the energy separation between suc-

*Electronic address: rtsaous@upatras.gr

cessive electronic levels is large compared to the thermal energy. Preliminary results have been presented in a conference form [15]. Deviations from the Wiedemann-Franz law in zero dimensional structures were predicted also in [19, 20] without, however, relating these to the possibility of an enhancement of ZT . Recently, an interesting prediction for a significant increase of ZT in a single-level molecule was made by Murphy *et al.* [16]. In Ref. [16] it was found that the energy parameter that controls ZT is the electron-electron repulsion. Here we show that for a multi-level system in the Coulomb blockade regime ZT is controlled by the level spacing and, consequently, the spatial confinement.

The Coulomb blockade oscillations of the conductance and thermopower in the sequential tunneling regime have been studied in the seminal papers by Beenakker [21] and by Beenakker and Staring [22]. Recently, the theory in [21, 22], that is based on a master equation approach within the constant interaction model, has been extended to calculate the electronic contribution to thermal conductance [14, 15, 19]. Here we present, for the first time, a detailed derivation for an analytical expression for κ_e which serves as a solid framework for the understanding of the behavior of this coefficient in the quantum limit. Within this framework we discuss the validity of previous results [19, 23]. The cases of a QD with equidistant and non-equidistant energy spectrum are examined. We also present detailed calculations and analytical derivations for the power factor S^2G and the figure of merit. We predict an optimization of the thermoelectric efficiency at specific values of the Fermi level. An important outcome of this work is the similarity in the temperature dependence of the electronic and phonon contribution to κ in structures with zero dimensional (0D) electrons and phonons. Our findings suggest the possibility of a dramatic increase in ZT in *both* electron- and phonon- blocking devices.

II. THEORY

We consider a quantum dot that consists of non-degenerate discrete energy levels ϵ_n ($n = 1, 2, 3, \dots$) weakly coupled to two electron reservoirs. In equilibrium both reservoirs have the same temperature T and the same chemical potential E_F . The energy distribution in the reservoirs is the Fermi-Dirac function $f(E - E_F) = 1/\{\exp[\beta(E - E_F)] + 1\}$, where $\beta = (k_B T)^{-1}$. We examine the Coulomb blockade regime where the charging energy $E_C = e^2/2C$ (C is the capacitance of the dot to the surroundings) is larger than the energy spacing $\Delta\epsilon$ between successive energy levels. The tunnel rate from level n to the left, L, (right, R,) reservoir is denoted as Γ_n^L (Γ_n^R). We assume that $k_B T$ and $\Delta\epsilon$ are much larger than $h(\Gamma_n^L + \Gamma_n^R)$ (where h is Planck's constant) and we neglect effects due the virtual tunneling (cotunneling) of electrons through the dot [21, 22].

The results presented here are based on the calculation

of the heat current Q through the dot when small temperature and voltage differences ΔT and ΔV , respectively, are applied between the two reservoirs. The linear response model proposed in the pioneer work by Beenakker [21] and Beenakker and Staring [22] for the calculation of the charge current J has been generalized to include Q [14, 15, 19]. Then Q is given by

$$Q = -\frac{\Gamma^L \Gamma^R}{\Gamma^L + \Gamma^R} \left(s_1 \frac{e\Delta V}{k_B T} + s_2 \frac{\Delta T}{k_B T^2} \right). \quad (2)$$

In the above equation the energy dependence of the tunnel rates has been ignored. e is the magnitude of the electron charge. Moreover, for the quantities s_m with $m = 0, 1, 2$ we use the following notation

$$s_m = \sum_{n=1}^{\infty} \sum_{N=1}^{\infty} P_{eq}(N) P_{eq}(\epsilon_n|N) [1 - f(E - E_F)] (E - E_F)^m \quad (3)$$

where, the sum indexes n and N refer to the energy level and the number of electrons in the dot, respectively, ϵ_n is the energy of the n state and $E = \epsilon_n + U(N) - U(N - 1)$ with $U(N)$ being the electrostatic energy for a dot with N electrons. Moreover, $P_{eq}(N)$ is the probability that the dot contains N electrons in equilibrium and $P_{eq}(\epsilon_n|N)$ is the probability that in equilibrium the n level is occupied given that the dot has N electrons. The expressions for $P_{eq}(N)$ and $P_{eq}(\epsilon_n|N)$ are given in [22].

Utilizing the standard transport equation [10]

$$Q = M\Delta V + K\Delta T \quad (4)$$

the transport coefficients M and K can be readily obtained [15], namely,

$$M = -\frac{e}{k_B T} \Gamma^{tot} s_1 \quad (5)$$

and

$$K = -\frac{1}{k_B T^2} \Gamma^{tot} s_2. \quad (6)$$

In the above equations $\Gamma^{tot} = \Gamma^L \Gamma^R / (\Gamma^L + \Gamma^R)$.

Onsager's symmetry relation relates the thermoelectric coefficient M to the thermopower S by $M = SGT$ [10]. Then S is written as

$$S = \frac{M}{GT} = -\frac{1}{eT} \frac{s_1}{s_0}, \quad (7)$$

where G is given by [21]

$$G = G_0 s_0, \quad (8)$$

with $G_0 = (e^2/k_B T) \Gamma^{tot}$. The expression (7) we derive for S is identical to the expression (3.13) obtained by Beenakker and Staring [22], where the authors calculated the electron current through the dot instead of the heat current. The approach we use here for S is the so-called Π -approach [10].

Finally, the electronic contribution to the thermal conductance can be calculated by using the standard relation [10]

$$\kappa_e = -K - S^2GT. \quad (9)$$

In Fig.1a we show the calculations of the thermoelectric coefficient M as a function of the Fermi level for a three-level QD when $\beta\Delta\epsilon = 10$ and $\Delta\epsilon = 0.5E_C$. M exhibits Coulomb blockade oscillations with periodicity $\Delta E_F = \Delta\epsilon + (e^2/C)$ as does the electrical conductance [21]. The effect of temperature on the shape of M is shown in Fig.1b. The Coulomb blockade oscillations of the coefficient K are shown in Fig.2a for the same parameters. As we can see $-K$ shows a double peak structure which is reproducible in energy intervals $\Delta\epsilon + (e^2/C)$. The theoretical values for K have been divided by L_0TG^{max} where $L_0 = (k_B/e)^2\pi^2/3$ and $G^{max} = G_0/4$ is the maximum value of the electrical conductance. The effect of temperature on the peaks of $-K$ is shown in Fig.2b and it will be explained by a simple analytical expression derived later.

In Fig.2 we have also shown the calculation of S^2GT . The curves for $-K$ and S^2GT are *indistinguishable* so that κ_e is near zero. It is found that the magnitude of the maximum values of κ_e collapses rapidly to zero as $(\beta\Delta\epsilon)^2 \exp(-\beta\Delta\epsilon)$ violating the Wiedemann-Franz law. Usually, in degenerate 2D and 1D systems S^2GT is a small quantity compared to $-K$ and the thermal conductance follows closely $-K$. The standard Sommerfeld expansion leads to the Wiedemann-Franz law according to which $\kappa_e = -K = L_0GT$. The above imposes a significant limitation on ZT when $S^2 < L_0$ even when the phonon contribution to the thermal conductance is ignored.

The similarity between $-K$ and S^2GT can be explained in simple terms. Namely, the dominant contribution to the summations over n and N in Eq. (3) occurs for $n = N = N_{min}$ where N_{min} is the integer which minimizes the absolute value of the energy difference $\Delta(N) = \epsilon_N + U(N) - U(N-1) - E_F$. We note that $\Delta(N_{min})$ oscillates in a sawtooth manner with E_F and passes through zero each time an electron enters the dot. In what follows we keep Beenakker's notation [21] and we write $\Delta(N_{min}) \equiv \Delta_{min}$. The oscillations of Δ_{min} are shown in Fig.3.

In the low- T limit the probabilities $P_{eq}(N_{min})$ and $P_{eq}(\epsilon_{N_{min}}|N_{min})$ can be approximated by [21]

$$P_{eq}(N_{min}) \approx f(\Delta_{min}) \quad (10)$$

and

$$P_{eq}(\epsilon_{N_{min}}|N_{min}) \approx 1 \quad (11)$$

Inspection of Eq. (3) shows that the quantities s_m can be written in the approximate form

$$s_m \approx s_m^{N_{min}} = f(\Delta_{min})[1 - f(\Delta_{min})](\Delta_{min})^m, \quad (12)$$

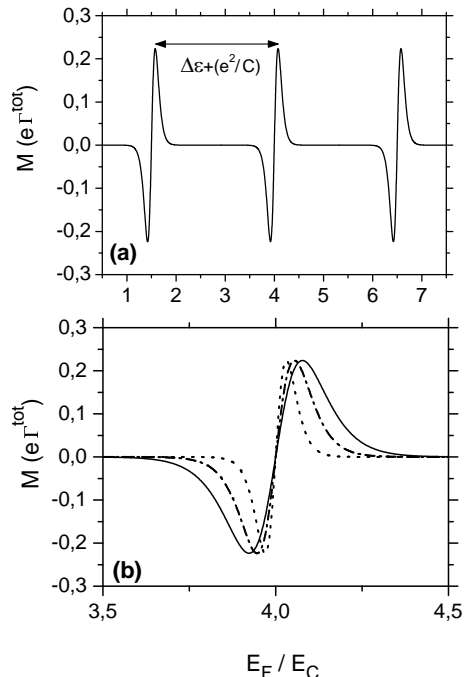


FIG. 1: The Coulomb blockade oscillations of M and the effect of temperature on the shape of M for a three-level dot. The solid line in (a) is for $k_B T = 0.05 E_C$. In (b) The solid, dashed-dotted and dotted lines correspond to $k_B T = 0.05, 0.035$ and $0.02 E_C$, respectively. The level spacing is $\Delta\epsilon = 0.5 E_C$.

where the superscript N_{min} denotes the contribution of the term $n = N_{min}$ in the sum (3). Now, by substituting Eq. (12) into Eqs.(5) and (6) one readily gets

$$S = \frac{M}{GT} = -\frac{1}{eT}\Delta_{min}, \quad (13)$$

and

$$S^2GT = -K = \frac{\Gamma^{tot}}{k_B T^2} f(\Delta_{min})[1 - f(\Delta_{min})](\Delta_{min})^2. \quad (14)$$

We recall that $f(\Delta_{min}) = 1/[\exp(\beta\Delta_{min}) + 1]$.

By maximizing Eq. (14) with respect to Δ_{min} we find that $-K$ and S^2GT exhibit two symmetric peaks at $\beta\Delta_{min} = \pm 2.4$ shown in Fig.2. The magnitude of the peaks is

$$(S^2GT)^{max} = 0.44k_B\Gamma^{tot}. \quad (15)$$

We note that the position of the two strong maxima are in agreement with the predicted maximization of S^2GT and ZT in materials with delta-like density of states [12]. Moreover, according to Eq. (13), the absolute magnitude of S that corresponds to the optimization of S^2GT is $2.4k_B/e = 207 \mu\text{V/K}$ which is in absolute agreement with the value predicted in [12].

At this point we should remark that Eq. (12) describes accurately the magnitude and the shape of the physical

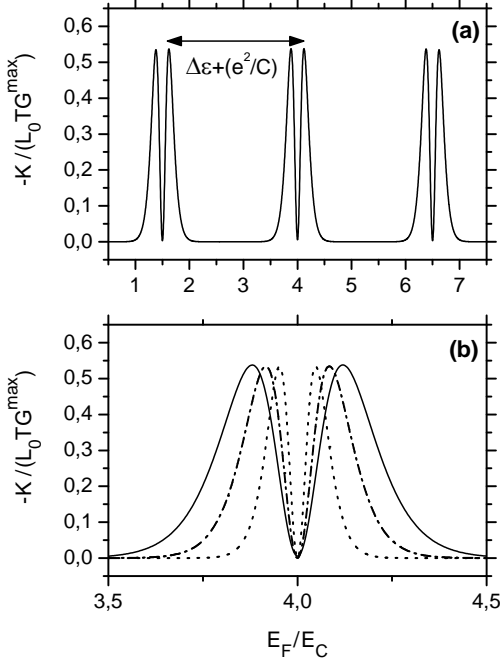


FIG. 2: The coefficient K as a function of E_F for a three-level dot. The calculated values of K are divided by $L_0 T G^{max}$ where $G^{max} = G_0/4$ is the maximum value of the conductance. In (a) the Coulomb blockade oscillations of K are shown for $k_B T = 0.05 E_C$. The effect of temperature on the shape of K is shown in (b). The solid, dashed-dotted and dotted lines correspond to $k_B T = 0.05, 0.035$ and $0.02 E_C$, respectively. The level spacing is $\Delta\epsilon = 0.5 E_C$. In the same figure we plot $S^2 GT$. The curves for $-K$ and $S^2 GT$ are indistinguishable.

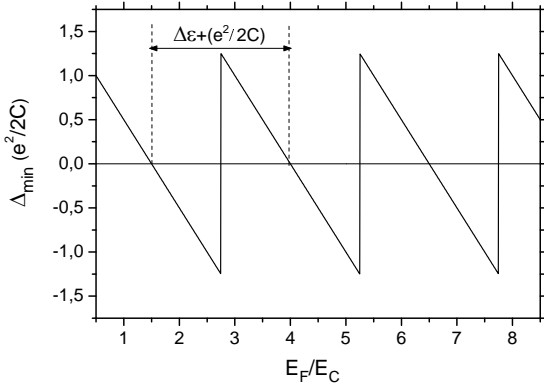


FIG. 3: The Coulomb blockade oscillations of Δ_{min} . $\Delta\epsilon = 0.5 E_C$.

quantities G , M , K and $S^2 GT$. Moreover, the expression (13) for S is in very good agreement with the numerical result around $\Delta_{min} = 0$ within the energy range $|\Delta_{min}| \lesssim \Delta E$. The contribution of the terms $n \neq N_{min}$ in Eq.(3) is responsible for the fine structure on the oscillations of S that was predicted by Beenakker and Staring

[22]. These terms do not affect $S^2 GT$ and are not discussed here for simplicity.

The strong competition between $-K$ and $S^2 GT$ in Eq.(9) gives $\kappa_e = 0$ if only the leading contribution to the sum (3) for $n = N_{min}$ and $N = N_{min}$ is considered. The terms that correspond to $n = N_{min} \pm 1$ disturb the above cancellation and, as we show below, an analytical expression for κ_e can be obtained. Inspection of Eqs.(3) and (10) shows that these terms introduce tiny corrections to the quantities s_m of the form

$$s_m^{N_{min} \pm 1} = P_{eq}(\epsilon_{N_{min} \pm 1} | N_{min}) (\Delta_{min} \pm \Delta\epsilon)^m \times f(\Delta_{min}) [1 - f(\Delta_{min} \pm \Delta\epsilon)] \quad (16)$$

where the superscripts $N_{min} \pm 1$ denote the contribution from the terms $n = N_{min} \pm 1$. The probabilities $P_{eq}(\epsilon_{N_{min} \pm 1} | N_{min})$ are given by [22]

$$P_{eq}(\epsilon_{N_{min}+1} | N_{min}) \approx \exp(-\beta\Delta\epsilon) \quad (17)$$

and

$$P_{eq}(\epsilon_{N_{min}-1} | N_{min}) \approx 1. \quad (18)$$

In the energy interval around $\Delta_{min} = 0$, which is the regime where G exhibits the well known peaks [21], $s_m^{N_{min} \pm 1}$ are smaller by a factor of $\exp(-\beta\Delta\epsilon)$ compared to $s_m^{N_{min}}$ given by Eq. (12) (we note that $\beta\Delta\epsilon \gg 1$). This explains why these corrections are unimportant for G [21]. To obtain κ_e we use Eq.(9) after we substitute K , S and G from Eqs.(6), (7) and (8), respectively. Then we take

$$\kappa_e = \frac{\Gamma^{tot}}{k_B T^2} \left[s_2 - \frac{(s_1)^2}{s_0} \right] \quad (19)$$

We, now, approximate s_m by the sum $s_m^{N_{min}} + s_m^{N_{min}-1} + s_m^{N_{min}+1}$ and we handle $s_m^{N_{min} \pm 1}$ as small quantities in order to linearize expression (19) by keeping terms up to first order in $\exp(-\beta\Delta\epsilon)$ and obtain

$$\kappa_e \approx \kappa_e^{N_{min}} + \kappa_e^{N_{min}+1} + \kappa_e^{N_{min}-1} \quad (20)$$

where,

$$\kappa_e^{N_{min}} = \frac{\Gamma^{tot}}{k_B T^2} \left(s_2^{N_{min}} - \frac{(s_1^{N_{min}})^2}{s_0^{N_{min}}} \right) = 0 \quad (21)$$

and

$$\begin{aligned} \kappa_e^{N_{min} \pm 1} &= \frac{\Gamma^{tot}}{k_B T^2} [s_2^{N_{min} \pm 1} \\ &+ \frac{s_1^{N_{min}}}{(s_0^{N_{min}})^2} (s_1^{N_{min}} s_0^{N_{min} \pm 1} - 2s_0^{N_{min}} s_1^{N_{min} \pm 1})]. \end{aligned} \quad (22)$$

The substitution of the quantities $s_m^{N_{min}}$ and $s_m^{N_{min} \pm 1}$ from Eqs.(12) and (16) gives

$$\begin{aligned} \kappa_e^{N_{min} \pm 1} &= k_B \Gamma^{tot} P_{eq}(\epsilon_{N_{min} \pm 1} | N_{min}) (\beta\Delta\epsilon)^2 \\ &\times f(\Delta_{min}) [1 - f(\Delta_{min} \pm \Delta\epsilon)] \end{aligned} \quad (23)$$

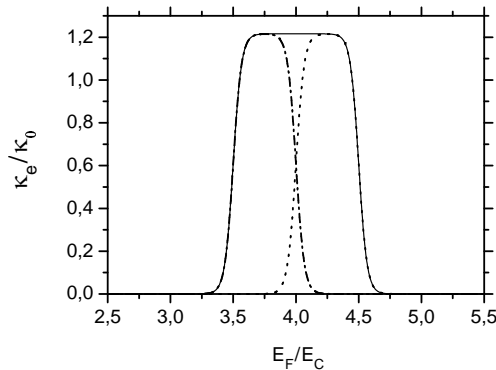


FIG. 4: The two symmetric contributions to κ_e (solid line) for a dot with equidistant energy spectrum around $\Delta_{min} = 0$. The dashed-dotted and the dotted lines correspond to $\kappa_e^{N_{min}-1}$ and $\kappa_e^{N_{min}+1}$, respectively. $\Delta\epsilon = 0.5E_C$ and $\beta\Delta\epsilon = 15$. $\kappa_0 = L_0TG^{max}(\beta\Delta\epsilon)^2 \exp(-\beta\Delta\epsilon)$ where $G^{max} = G_0/4$. The shown structure is reproducible in energy intervals $\Delta\epsilon + (e^2/C)$ except for the first and the last level where κ_e is $\kappa_e^{N_{min}+1}$ and $\kappa_e^{N_{min}-1}$, respectively.

It is apparent from the above analysis that κ_e consists of two contributions

$$\kappa_e \approx \kappa_e^{N_{min}+1} + \kappa_e^{N_{min}-1}. \quad (24)$$

These contributions are shown as dashed-dotted and dotted lines in Fig.4. We see that they are symmetric around $\Delta_{min} = 0$ and peak at $\Delta_{min} = -\Delta\epsilon/2$ and $\Delta\epsilon/2$. We note that $\kappa_e^{N_{min}+1}$ and $\kappa_e^{N_{min}-1}$ are periodic as a function of E_F with periodicity $\Delta\epsilon + (e^2/C)$.

We should mention that there is a symmetry in the correction terms $G^{N_{min}\pm 1}$ for the electrical conductance, arising from the terms $n = N_{min} \pm 1$, and $\kappa_e^{N_{min}\pm 1}$. Namely,

$$\kappa_e^{N_{min}\pm 1} = \left(\frac{k_B}{e}\right)^2 T(\beta\Delta\epsilon)^2 G^{N_{min}\pm 1}. \quad (25)$$

Such a symmetry was absent in the papers [19, 23]. This poses a question about the existence of a solid theoretical background for the expressions for κ_e that appeared in these papers and about the validity of the relevant results especially for the case of a dot with degenerate energy spectrum.

Substituting Eq.(23) in (24), after some trivial algebra we take [14, 15]

$$\begin{aligned} \kappa_e &= k_B \Gamma^{tot}(\beta\Delta\epsilon)^2 \\ &\times \frac{(1 + e^{\beta\Delta\epsilon})e^{\beta\Delta_{min}}}{e^{\beta\Delta\epsilon}(e^{2\beta\Delta_{min}} + 1) + e^{\beta\Delta_{min}}(e^{2\beta\Delta\epsilon} + 1)}. \end{aligned} \quad (26)$$

Eq. (26) is in excellent agreement with the numerical result. The magnitude of the peak values of κ_e around $\Delta_{min} = 0$ is given by the simple expression

$$\kappa_e \approx k_B \Gamma^{tot}(\beta\Delta\epsilon)^2 \exp(-\beta\Delta\epsilon). \quad (27)$$

In deriving the above equation we have taken into account that $\exp(\beta\Delta\epsilon) \gg 1$ in the quantum limit. Eq. (27) denotes a strong sensitivity of κ_e to the details of the energy spectrum.

Inspection of Eqs.(8) and (27) shows that the Wiedemann-Franz law is not valid in the quantum limit. We find that the peak values of the Coulomb blockade oscillations of κ_e are smaller than that the Wiedemann-Franz law predicts by a factor of the order $(\beta\Delta\epsilon)^2 \exp(-\beta\Delta\epsilon)$. Namely, the ratio of the peak values of κ_e and G for $\Delta_{min} = 0$ is given by

$$\frac{\kappa_e^{max}}{G^{max}} = \frac{12}{\pi^2} L_0 T (\beta\Delta\epsilon)^2 \exp(-\beta\Delta\epsilon). \quad (28)$$

As we show below the violation of the Wiedemann-Franz law in the system under consideration leads to an exponential increase of ZT with $\beta\Delta\epsilon$. Also, recently it has been reported that deviations from the Wiedemann-Franz law lead to enhancement of ZT in nanocontacts made of two-capped single wall nanotubes [24], quantum dots attached to ferromagnetic leads [18], and strongly correlated quantum dots[25].

The maximization of S^2GT , discussed earlier, has a direct impact on the dimensionless figure of merit ZT when the phonon contribution to the thermal conductance is ignored

$$ZT = \frac{S^2GT}{\kappa_e}. \quad (29)$$

According to the above expression and Eqs.(15) and (27) ZT shows two strong maxima at $\beta\Delta_{min} = \pm 2.4$ of magnitude

$$(ZT)^{max} = \frac{(S^2GT)^{max}}{\kappa_e} = 0.44 \exp(\beta\Delta\epsilon)/(\beta\Delta\epsilon)^2. \quad (30)$$

The structure of ZT is shown in Fig.5c. The exponential dependence of these maxima can be readily explained by the fact that, in the energy interval where S^2GT exhibits the peak structure shown in Fig.5a, κ_e remains constant and its magnitude is given by Eq. (27) (see Fig.5b).

Eq. (30) shows that the thermoelectric efficiency can be dramatically enhanced by controlling the size of the dot and consequently $\Delta\epsilon$. For small dots (or molecules) the requirement that the system is in the quantum limit is fulfilled even at room temperature. Practically speaking, the quantum limit is approached when $\beta\Delta\epsilon \geq 5$. High values of ZT in the range of 2.6 to 97 at $T = 300$ K ($k_B T = 0.026$ eV) can be obtained when $\Delta\epsilon$ varies between 5 to 10 $k_B T$ (namely, between 0.13 to 0.26 eV). We note that the energy separation between the first two energy levels in a spherical dot for a material with electron effective mass of the order of 0.1 m_e (m_e is the electron mass) is greater than 0.15 eV when the diameter is less than 5 nm. Finally, we add that in our model we have assumed that the charging energy E_C is larger than $\Delta\epsilon$. Large values of E_C of the order of the tenth of eV have

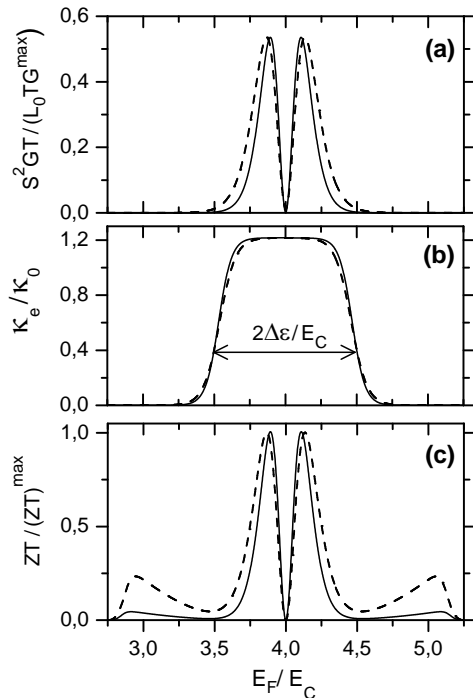


FIG. 5: Calculated values of S^2GT , κ_e and ZT as a function of E_F for a three-level dot. The level spacing is $\Delta\epsilon = 0.5E_C$. The solid and dashed lines correspond, respectively, to $\beta\Delta\epsilon=11$ and 9. The results are plotted around $E_F = 4E_C$ that corresponds to $\Delta_{min} = 0$ when an electron enters the dot at the level $n = 2$. In (b) $\kappa_0 = L_0TG^{max}(\beta\Delta\epsilon)^2 \exp(-\beta\Delta\epsilon)$ where $G^{max} = G_0/4$ and in (c) $(ZT)^{max} = 0.44 \exp(\beta\Delta\epsilon)/(\beta\Delta\epsilon)^2$.

been reported recently in single-electron transistors with organic molecules acting as Coulomb islands[26, 27].

In a recent paper [23] the possibility of tuning ZT of a dot by varying E_F was recognized. In [23] no detailed calculations were performed and the possibility of tuning ZT was incorrectly related solely to the dependence of κ_e on the energy spectrum and the variation of κ_e with E_F . However, the variation of S^2GT with E_F is the most remarkable behavior predicted in these systems. Although, the phonon contribution to the thermal conductance could washout the variation of the total thermal conductance as a function of E_F , ZT will still vary periodically with E_F following the structure of S^2GT shown in Figs.2 and 5a. Moreover, the maximization of S^2GT could be utilized for the prediction of an optimal value for κ_{ph} that maximizes ZT [16].

So far our analysis has referred to a dot with equidistant energy levels. The generalization to a non-equidistant energy spectrum is straightforward. However, we should remark that this generalization will not affect our findings for S^2GT (apart from the absence of a regular periodicity in the oscillations of S^2GT) but it will only affect the shape of ZT in the case where the phonon contribution to thermal conductance is small compared

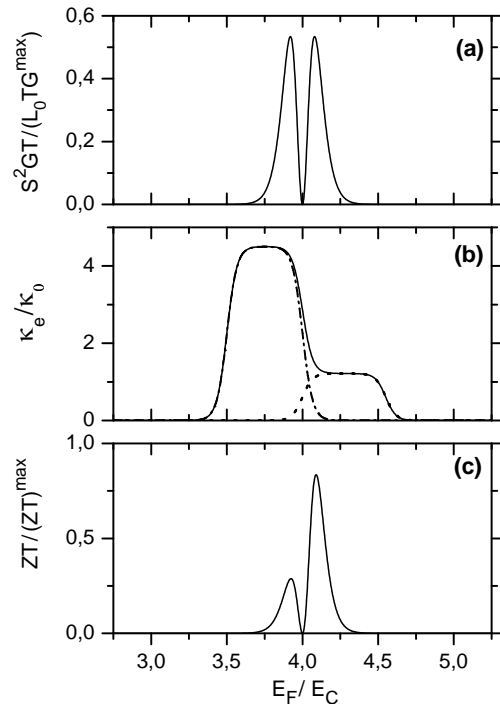


FIG. 6: Calculated values of S^2GT , κ_e and ZT as a function of E_F for a dot with non-equidistant energy spectrum. The results are plotted around $E_F = 4E_C$ that corresponds to $\Delta_{min} = 0$ when an electron enters the dot at the level $n = 2$. The energy separation between the two adjacent levels is $\Delta\epsilon_{pr} = 0.5E_C$ and $\Delta\epsilon_{ne} = 0.55E_C$. $\beta\Delta\epsilon_{pr} = 15$ and $\beta\Delta\epsilon_{ne} = 16.5$. The dashed-dotted and the dotted lines in (b) show the contributions $\kappa_e^{N_{min}-1}$ and $\kappa_e^{N_{min}+1}$, respectively. $\kappa_0 = L_0TG^{max}(\beta\Delta\epsilon_{ne})^2 \exp(-\beta\Delta\epsilon_{ne})$ and $(ZT)^{max} = 0.44 \exp(\beta\Delta\epsilon_{ne})/(\beta\Delta\epsilon_{ne})^2$.

to κ_e . This is due to the profound effect of the energy spectrum on the shape of κ_e . In Fig.6 we present calculations for S^2GT , κ_e and ZT for a three-level dot when one electron enters the dot at the level $n = 2$. The energy separation between the next and the previous energy level is $\Delta\epsilon_{ne} = 0.55E_C$ and $\Delta\epsilon_{pr} = 0.5E_C$. To obtain κ_e in the case of dot with non-equidistant energy spectrum one needs to replace $\Delta\epsilon$ by $\Delta\epsilon_{ne}$ and $\Delta\epsilon_{pr}$ in the expressions (23) for $\kappa_e^{N_{min}+1}$ and $\kappa_e^{N_{min}-1}$, respectively. In this case the two contributions to κ_e become asymmetric as shown by the dashed-dotted and dotted lines in Fig.6b. This results to the two asymmetric peaks in ZT shown in Fig.6c.

We should remark at this point that the phonon contribution to thermal conductance could significantly suppress ZT . However, the phonon confinement in free-standing QDs or QDs embedded in a matrix material, where there is a significant mismatch in the elastic properties of the QD and the surrounding material, could dramatically decrease the phonon contribution κ_{ph} . The 3D confinement of phonons in nano-objects results in similar restrictions in the phase space of the phonon wave

vector as in the case of electrons. The discrete phonon frequency spectrum influences the phonon heat transfer through a nanostructure. In what follows we will attempt to reveal the similarities between the fermionic and the bosonic contributions to the thermal conductance. As we will show both contributions show an activated behavior.

We start from the Landauer expression used by Rego and Kirczenow [28] for the heat transferred by 1D ballistic phonons through a quantum wire attached to two thermal reservoirs in the presence of a small temperature difference ΔT between them. This is modified here to account for the discrete phonon spectrum of the QD. We assume that the temperature in the right reservoir is raised by ΔT compared to the temperature in the left reservoir. Then the phonon contribution to the heat flow from the right to the left reservoir is written in the form [29]

$$Q_{ph} = \sum_i \int d\omega \hbar\omega T_i(\omega) [n_R(\omega) - n_L(\omega)] \quad (31)$$

where $T_i(\omega)$ denotes the transmission coefficient for a phonon of frequency ω through the i th-mode into the nanostructure and $n_R(\omega) = \{\exp[\frac{\hbar\omega}{k_B(T+\Delta T)}] - 1\}^{-1}$ and $n_L(\omega) = \{\exp(\frac{\hbar\omega}{k_B T}) - 1\}^{-1}$ are the phonon distribution functions in the right and the left reservoirs, respectively. The summation is over all the vibrational modes. For the case of resonance energy transfer we write the transmission coefficient $T_i(\omega)$ in the form [30]

$$T_i(\omega) = \frac{\Gamma_{ph}^L \Gamma_{ph}^R}{\Gamma_{ph}^L + \Gamma_{ph}^R} \delta(\omega - \omega_i) \quad (32)$$

where Γ_{ph} denotes the phonon tunnel rate. Then we take

$$Q_{ph} = \sum_i \hbar\omega_i \Gamma_{ph}^{tot} [n_R(\omega_i) - n_L(\omega_i)], \quad (33)$$

where $\Gamma_{ph}^{tot} = \Gamma_{ph}^L \Gamma_{ph}^R / (\Gamma_{ph}^L + \Gamma_{ph}^R)$. The expression (33) is in agreement with the expression derived recently by Segal and Nitzan [30] for the heat current through a harmonic molecule weakly coupled to two thermal reservoirs by using a master equation approach.

In the linear regime, where ΔT is small, it can be easily shown that

$$n_R(\omega_i) - n_L(\omega_i) = -\hbar\omega_i \frac{\partial n_L(\omega_i)}{\partial(\hbar\omega_i)} \frac{\Delta T}{T}, \quad (34)$$

where,

$$\frac{\partial n_L(\omega_i)}{\partial(\hbar\omega_i)} = -\beta \frac{\exp(\beta\hbar\omega_i)}{[\exp(\beta\hbar\omega_i) - 1]^2}. \quad (35)$$

At temperatures where $\beta\hbar\omega_i \gg 1$ we can write

$$\frac{\partial n_L(\omega_i)}{\partial(\hbar\omega_i)} \approx -\beta \exp(-\beta\hbar\omega_i) \quad (36)$$

Then, the phonon contribution to the thermal conductance $\kappa_{ph} = Q_{ph}/\Delta T$ is written in the form

$$\kappa_{ph} = k_B \sum_i \Gamma_{ph}^{tot} (\beta\hbar\omega_i)^2 \exp(-\beta\hbar\omega_i). \quad (37)$$

At low T only the first low energy phonon mode $\hbar\omega_0$ contributes significantly to κ_{ph} . Then we can write

$$\kappa_{ph} = k_B \Gamma_{ph}^{tot} (\beta\hbar\omega_0)^2 \exp(-\beta\hbar\omega_0). \quad (38)$$

The similarity of the above expression with Eq.(27) for κ_e is quite remarkable. Interestingly, as in the case of the 1D thermal conductance [28], the phononic and the electronic contributions to the thermal conductance in structures with a 3D electron and phonon confinement appear to show a similar T -behavior.

According to our analysis the maximum value for ZT is

$$(ZT)^{max} = \frac{0.44k_B \Gamma^{tot}}{\kappa_e + \kappa_{ph}} \quad (39)$$

where κ_e and κ_{ph} are given by Eqs.(27) and (38). Due to the activated terms in these equations ZT can take values much larger than 1. Our finding suggests that the control of the electron and phonon confinement effects in nanostructures can improve significantly their thermoelectric properties. Namely, for $\hbar\omega_0$ and $\Delta\epsilon$ of the order of 150 to 200 meV and $\Gamma^{tot} \approx \Gamma_{ph}^{tot}$ we find that ZT can reach the values 2.2 to 8.4 at $T = 300$ K. We also note that $(ZT)^{max}$ is an increasing function of $\Gamma^{tot}/\Gamma_{ph}^{tot}$.

III. CONCLUSIONS

In summary, we have presented a comprehensive study of the thermoelectric coefficients of a multi-level QD weakly coupled to two electron reservoirs in the Coulomb blockade regime for sequential tunneling. Our analysis focuses on the quantum limit[21] where the level spacing between successive electronic levels is much larger than the thermal energy ($\beta\Delta\epsilon \gg 1$). Analytical expressions for the power factor and the figure of merit are derived. We found an exponential increase of ZT with $\beta\Delta\epsilon$ when phonons are ignored. This is due to the activated behavior of κ_e . We also show that κ_{ph} for a dot with discrete phonon spectrum shows a similar activated behavior. Interestingly both fermionic and bosonic contributions to the thermal conductance show a very similar T -dependence. Although, it was previously believed that electron-transmitting and phonon-blocking structures have good thermoelectric properties [3], our results now open a route for designing electron-blocking and phonon-blocking nanostructures with improved thermoelectric performance.

-
- [1] M. S. Dresselhaus, G. Chen, M. Y. Tang, R. G. Yang, H. Lee, D. Z. Wang, Z. F. Ren, J.-P. Fleurial, and P. Gogna, *Adv. Mater.* **19**, 1043 (2007).
- [2] A. Majumdar, *Science* **303**, 777 (2004).
- [3] R. Venkatasubramanian, E. Siivola, T. Colpitts, and B. O'Quinn, *Nature* **413**, 597 (2001).
- [4] T. C. Harman, P. J. Taylor, M. P. Walsh, and B. E. LaForge, *Science* **297**, 2229 (2002).
- [5] K. F. Hsu, S. Loo, F. Guo, W. Chen, J. S. Dyck, C. Uher, T. Hogan, E. K. Polychroniadis, and M. G. Kanatzidis, *Science* **303**, 818 (2004).
- [6] B. Poudel, Q. Hao, Y. Ma, Y. Lan, A. Minnich, B. Yu, X. Yan, D. Wang, A. Muto, D. Vashaee, X. Chen, J. Liu, M. S. Dresselhaus, G. Chen, and Z. Ren, *Science* **320**, 634 (2008).
- [7] A. I. Hochbaum, R. Chen, R. D. Delgado, W. Liang, E. C. Garnett, M. Najarian, A. Majumdar, and P. Yang, *Nature* **451**, 163 (2008).
- [8] A. I. Boukai, Y. Bunimovich, J. Tahir-Kheli, J. -K. Yu, W. A. Goddard III, and J. R. Heath, *Nature* **451**, 168 (2008).
- [9] R. Fletcher, E. Zaremba, and U. Zeitler in *Electron-Phonon Interactions in Low Dimensional Structures*, edited by L. Challis (Oxford University Press, Oxford, 2003), p. 149.
- [10] M. Tsaousidou in *The Oxford Handbook of Nanoscience and Technology*, edited by A.V. Narlikar and Y.Y. Fu, Vol.II, Ch.13, (Oxford University Press, Oxford, 2010), p.477.
- [11] L. D. Hicks and M. S. Dresselhaus, *Phys. Rev. B* **47**, 12727 (1993); L. D. Hicks and M. S. Dresselhaus, *Phys. Rev. B* **47**, 16631 (1993).
- [12] G. D. Mahan and J. O. Sofo, *Proc. Natl. Acad. Sci. USA* **93**, 7436 (1996).
- [13] T. E. Humphrey and H. Linke, *Phys. Rev. Lett.* **94**, 096601 (2005).
- [14] M. Tsaousidou and G. P. Triberis, arXiv:cond-mat/0605286 (May 2006).
- [15] M. Tsaousidou and G. P. Triberis, in *Physics of Semiconductors: 28th International Conference on the Physics of Semiconductors-ICPS 2006*, AIP Conf. Proc. **893** (AIP, New York 2007) p. 801-802.
- [16] P. Murphy, S. Mukerjee, and J. Moore, *Phys. Rev. B* **78**, 161406(R) (2008).
- [17] C. M. Finch, V. M. García-Suárez, and C. J. Lambert, *Phys. Rev. B* **79**, 033405 (2009).
- [18] R. Świrkowicz, M. Wierzbicki, and J. Barnaś, *Phys. Rev. B* **80**, 195409 (2009).
- [19] X. Zianni, *Phys. Rev. B* **75**, 045344 (2007).
- [20] B. Kubala, J. König, and J. Pekola, *Phys. Rev. Lett.* **100**, 066801 (2008).
- [21] C. W. J. Beenakker, *Phys. Rev. B* **44**, 1646 (1991).
- [22] C. W. J. Beenakker and A. A. M. Staring, *Phys. Rev. B* **46**, 9667 (1992).
- [23] X. Zianni, *Phys. Rev. B* **78**, 165327 (2008).
- [24] K. Esfarjani, M. Zebarjadi, and Y. Kawazoe, *Phys. Rev. B* **73**, 085406 (2006).
- [25] T. A. Costi and V. Zlatić, *Phys. Rev. B* **81**, 235127 (2010).
- [26] Y. Wakayama, T. Kubota, H. Suzuki, T. Kamikado, and S. Mashiko, *Journal of Appl. Phys.* **94**, 4711 (2003).
- [27] Y. Wakayama, T. Kubota, H. Suzuki, T. Kamikado, and S. Mashiko, *Nanotechnology* **15**, 1446 (2004).
- [28] L. G. C. Rego and G. Kirczenow, *Phys. Rev. Lett.* **81**, 232 (1998).
- [29] A. Ozpineci and S. Ciraci, *Phys. Rev. B* **63**, 125415 (2001).
- [30] D. Segal and A. Nitzan, *Phys. Rev. Lett.* **94**, 034301 (2005).